Ingredients of the planet-formation puzzle: Gas substructures and kinematics in transition discs

Wölfer, L.B.

Equipped with his five senses,
man explores the universe around him
and calls the adventure science.

Edwin Powell Hubble

Chapter 1

Introduction

Since time immemorial, people have wondered about the origin and structure of our world as well as our place in the cosmos. How did the Earth form and which laws of nature does it follow? Are we alone, sitting on a tiny oasis surrounded by lifeless wasteland, or does life flourish in many corners of the universe? First observations of the night sky were captured already in the earliest history of humanity in the form of cave paintings and over centuries better instruments reaching far beyond the human eye were developed. Nowadays, there exist remarkable observatories both on Earth and in space that are capable of resolving the cosmos even on its smallest scales. At the same time, dedicated theoretical efforts have invoked mechanisms to explain the physics behind the observations. The question of extraterrestrial life reached a new era when the first exoplanet – a planet orbiting another star than our Sun – was discovered in 1992 (Wolszczan & Frail 1992) around a pulsar and in 1995 around a solar-type star (Mayor & Queloz 1995). To date, 5323 exoplanets[1] have been confirmed through various detection techniques, a number that is steadily growing and will be outdated already by the time you read this thesis. These planetary systems appear to come in an enormous variety, including the stellar and planetary masses or sizes but also the system architectures in terms of the number, species, or distribution of planets. In this comparison, the Solar System itself presents to be rather atypical (e.g., Raymond et al. 2020), raising questions of whether there may be an observational bias or if the occurrence of life itself is uncommon. To understand the formation of planets and the diversity of developed planetary systems, it is crucial to take a step back and set the focus on their nursery stages in the circumstellar material. Here, dense remnants of the star formation process called protoplanetary or planet-forming discs provide the gaseous and dusty building blocks to assemble planets. These discs are not static objects but they evolve and eventually disperse over time with the evolutionary processes not only shaping the disc's appearance but also influencing (and putting a limit on) the planet-formation mechanisms. Vice versa, planets

[1] `http://www.exoplanet.eu`, as of 26 February 2023

interact with their environment, impact disc evolution, and are expected to alter their host disc's structure, for example in terms of density, temperature, or velocity. Even though such young embedded planets may be hidden from the direct eye of our telescopes, their planet–disc interactions still leave marks observable to us depending on their mass and location. Modelling the dynamic processes taking place in discs together with characterizing the observed substructures represent key pieces in assembling the planet-formation puzzle.

1.1 Star and planet formation

Stars are formed in giant molecular clouds, an interstellar accumulation of mainly molecular hydrogen gas (H_2) and some small sub-μm-sized dust grains, which make up only about 1 % of the total mass (Draine 2003). Under certain conditions, the dense ($n > 10^4\,\mathrm{cm}^{-3}$) and cold ($T \sim 10 - 20\,\mathrm{K}$) cores of these clouds can collapse under their own gravity, forming a prestellar core in the centre (e.g., review of Evans 1999). In the subsequent evolution, young stellar objects (YSOs) are theoretically divided into four evolutionary stages (Shu et al. 1987) and observationally categorized into four classes based on the spectral slope of their spectral energy distribution (SED; Lada 1987; André et al. 1993; Greene et al. 1994; Fig. 1.1). In this context, infrared to submillimetre wavelengths are usually best to identify the class of a YSO: High-energy radiation from the star (UV and optical) heats the surrounding dust which re-emits at lower energies and consequently longer wavelengths. The four theoretical stages and observed classes roughly correspond to each other, but it is important to note that the SED depends on the geometry of the protostellar system such as the inclination (e.g., Crapsi et al. 2008) and thus deviations may occur.

In the initial stage after the formation of the prestellar core, the latter has collapsed into a protostar surrounded by an infalling envelope (Stage 0). At the same time, a disc begins to form around the protostar due to angular momentum conservation. Stage 0 is marked by a high envelope mass that significantly exceeds the stellar mass. The emission of a Class 0 YSO is thus dominated by the envelope. In the following, the mass of the protostar increases due to accretion, and it grows larger than the envelope mass within $\sim 10^5\,\mathrm{yr}$ (Stage I). As the envelope begins to dissipate both due to accretion and bipolar outflows, emission from the star and disc starts to become visible (Class I). These processes continue and after $\sim 10^5 - 10^6\,\mathrm{yr}$, the embedded star formation stage is over, and instead, a pre-main-sequence star surrounded by a gas-rich protoplanetary disc (Stage II) has formed. The SED is marked by strong stellar emission, the disc appears to be optically thick in the infrared and mostly optically thin in the millimetre-regime (Class II). After $\sim 10^6 - 10^7\,\mathrm{yr}$, accretion ceases and the disc material has grown into planets and smaller bodies or dissipated due to processes such as disc winds. In this Stage III, the star is surrounded by a gas-poor debris disc containing dust created by collisions of larger bodies. The SED is dominated by the black body radiation of the pre-main-sequence star (Class III). Finally, the disc vanishes, the star enters the main sequence and a fully developed stellar system is born. This

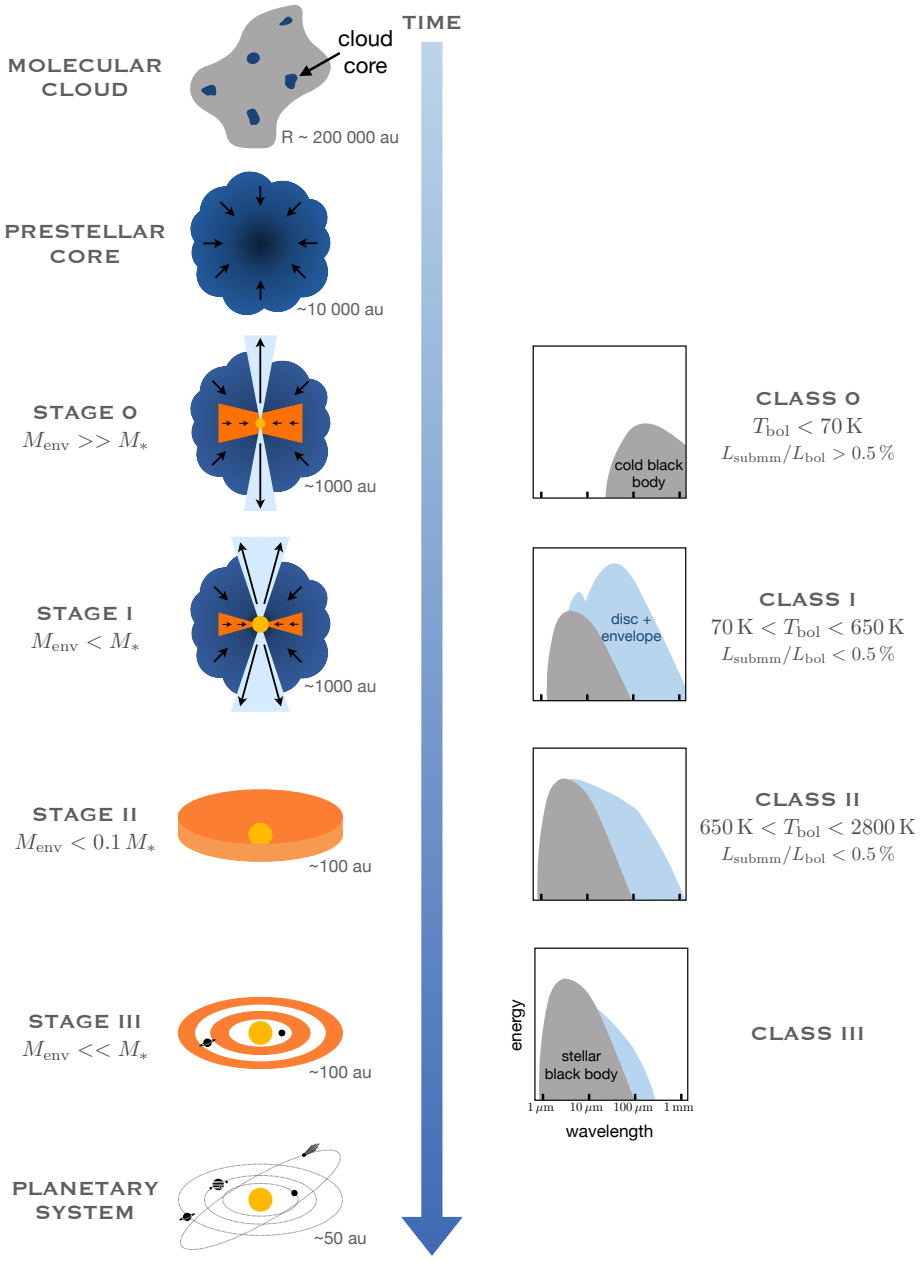

Figure 1.1: Schematic overview of the different theoretical stages (left) and observational classes based on the SED (right) of star formation. The focus of this thesis are Class II objects, which are also known as protoplanetary discs.

thesis focuses on the second evolutionary stage where substructures in the gas disc can be observed with the Atacama Large Millimeter/submillimeter Array (ALMA; ALMA Partnership et al. 2015) and analysed in the context of their (possibly dynamical) origins.

1.2 Protoplanetary discs

Circumstellar discs are a natural outcome of the planet-formation process. During the gravitational collapse of a rotating cloud core, the lowest angular momentum material falls towards the centre, forming a protostar as density and temperature rise (e.g., Terebey et al. 1984; Yorke et al. 1993), while the highest angular momentum material distributes into a rotating accretion disc from which the protostar is feeding during the first few million years of its lifetime. As a consequence, the protoplanetary disc contains only a small mass fraction ($10^{-1} - 10^{-4}\,M_*$; Manara et al. 2022) compared to the total mass of the system, but most of the angular momentum is deposited therein. Such a Keplerian disc is hydrodynamically stable (Drazin & Reid 1981; Ruden 1993) and without a mechanism to decrease angular momentum, the particles would just continue to orbit the central star at the same radius instead of spiralling inwards to be accreted. Thus, for a protoplanetary disc to evolve, angular momentum needs to be either lost from the system entirely or redistributed within the disc. Such processes, described further in the following section, occur on timescales much larger than the orbital or dynamical timescale, hence protoplanetary discs represent dynamically long-lived structures which evolve and eventually disperse slowly over a timescale of a few million years.

1.2.1 Disc evolution

Two, not mutually exclusive, processes have been proposed to be the main drivers of global disc evolution: Magnetically-driven disc winds (MHD disc winds) and viscous stresses. The latter are believed to play an especially important role during the earlier stages of a still massive circumstellar disc, while disc winds start to dominate at later phases when the viscous accretion rates drop below the wind mass-loss rates. In the classical picture, the disc is described as a vertically thin and axisymmetric sheet of viscous fluid. A shear between two adjacent gas annuli causes the redistribution of angular momentum, meaning that the inner disc loses angular momentum to the outer disc (e.g., Shakura & Sunyaev 1973; Lynden-Bell & Pringle 1974; Pringle 1981; Hartmann et al. 1998). As a consequence of angular momentum conservation, the outermost disc regions expand to larger radii, a process known as viscous spreading, while the innermost regions move towards the star where they can be accreted.

The source of viscosity remains a matter of active debate, but it is known that molecular viscosity caused by random motions of gas particles is too low to account for the observed lifetimes of protoplanetary discs (Armitage 2019). Instead, a viscously evolving disc is proposed to be turbulent (Shakura & Sunyaev 1973). One mechanism commonly invoked to be the dominant driver of turbulence

in discs is the magneto-rotational instability (MRI; Balbus & Hawley 1991), which can occur in weakly magnetized but sufficiently ionized discs. Other mechanisms include the vertical shear instability (VSI; Richard & Zahn 1999; Nelson et al. 2013; Stoll & Kley 2014) or gravitational instabilities (Lin & Pringle 1987), where spiral density waves redistribute angular momentum. For simplicity, it is usually assumed that the viscosity is constant across the disc, however, this is unlikely physical. The MRI for example is expected to be suppressed in the so-called dead zones (e.g., Blaes & Balbus 1994; Sano & Stone 2002; Turner et al. 2010; Flock et al. 2015), disc regions of low ionization, which stand in contrast to a uniform viscosity. Regardless of the exact origin, assuming a constant viscosity brings the advantage that the disc evolution can be described by a single dimensionless parameter α in the so-called α-prescription

$$\nu \equiv \alpha \frac{c_\mathrm{s}^2}{\Omega_\mathrm{K}} = \alpha c_\mathrm{s} H, \tag{1.1}$$

which was introduced by Shakura & Sunyaev (1973). Here, c_s is the isothermal sound speed, Ω_K the Keplerian orbital frequency, $H = c_\mathrm{s}/\Omega_\mathrm{K}$ the vertical pressure scale height, and α describes the efficiency of angular momentum transport due to turbulence.

In contrast to viscous evolution, a disc-wind-driven evolution represents an external way to remove angular momentum (and mass) and does not require turbulence. In the presence of a magnetic field, a magnetic disc wind can be launched from the disc surface by the magneto-centrifugal force if the poloidal field lines are inclined at a sufficiently large angle from the rotation axis (e.g., Blandford & Payne 1982; Pascucci et al. 2022). The accelerated material consequently carries away angular momentum, causing the remaining material to lose angular momentum and move inwards. Models have indeed shown that such magnetic disc winds can efficiently remove the angular momentum required to drive the stellar accretion (e.g., Ferreira et al. 2006; Béthune et al. 2017; Zhu & Stone 2018; Tabone et al. 2022a,b).

Despite being nearly ubiquitously invoked in the context of disc evolution, observational evidence for both (strong) turbulence in discs and magnetic disc winds is scarce. Understanding what modulates angular momentum transport in discs, influencing their lifetime and thus the time planetary systems have to form, represents one of the major missing pieces of the planet-formation puzzle.

1.2.2 Disc dispersal

While the simple theory of viscous evolution described in the previous section can roughly account for the observed morphology and physical properties of protoplanetary discs, it however predicts a decelerated dispersal where the disc becomes steadily fainter at all wavelengths, resulting in a long final phase of homogeneous fading. Since evidence for such slowly draining discs is lacking, other mechanisms which rapidly deplete the disc at advanced stages must be at play and result in a much shorter dispersal time, which (according to observations) makes up only

about 10 % of the total disc lifetime. Among these mechanisms is photoevaporation, which is believed to play a significant role and is detailed in the following.

1.2.2.1 Photoevaporation

Photoevaporation describes the phenomenon when high-energy stellar photons (either internal or external) irradiate, and consequently heat, the upper protoplanetary disc layers until the thermal energy exceeds the gravitational binding energy and a thermal wind is centrifugally launched from the surface at a given radius (see reviews of Hollenbach et al. 2000; Clarke 2011; Alexander et al. 2014; Gorti et al. 2016; Ercolano & Pascucci 2017; Pascucci et al. 2022). YSOs typically show vigorous accretion and thus photoevaporation is thought to take over the disc's evolution at later stages when the accretion rate has considerably dropped, then initialising a fast inside-out clearing. In a simplified picture, schematically shown in Fig. 1.2 (adapted from Ercolano & Pascucci 2017), the disc evolves through three main stages: As previously mentioned, for most of the disc's lifetime, the evolution is governed by viscosity (Stage 1). Even though photoevaporation may already be responsible for a small amount of mass loss, the latter is dominated by viscous accretion, meaning that the surface density is only marginally influenced by photoevaporation during the first few million years. Both the surface density and mass accretion rate gradually decrease over time, resulting in a lower opacity which enables the radiation to penetrate into deeper disc layers. At some point, the accretion rate drops below the wind mass-loss rate ($\dot{M}_{\rm acc} < \dot{M}_{\rm w}$) and photoevaporation begins to dominate the mass loss. Beyond the so-called gravitational radius

$$R_{\rm g} = \frac{GM_*}{c_{\rm s}^2}, \tag{1.2}$$

inwards flowing parcels are blown away with the wind rather than reaching the inner disc regions to be accreted. As a result, the replenishment of mass inside of $R_{\rm g}$ is prevented and an annular gap or cavity is formed, that fully detaches the inner and outer disc regions from each other (Stage 2). Now isolated from matter resupply, the inner disc is rapidly accreted onto the central star within 10^5 years. The outer disc on the other hand is being illuminated directly (Alexander et al. 2006a,b) and quickly erodes in an outwards direction (Stage 3). This final phase of disc dispersal appears within a few 10^5 years (Clarke 2011; Gorti & Hollenbach 2009) and thus the evolution of protoplanetary discs is also called a two-timescale behaviour.

The exact location and time of gap opening depends on the spectrum of the irradiating photons and there is an ongoing debated in the literature about what type of radiation may be the main driver of photoevaporative winds: Far-ultraviolet radiation (FUV; $6\,\mathrm{eV} < h\nu < 13.6\,\mathrm{eV}$), extreme-ultraviolet radiation (EUV, $13.6\,\mathrm{eV} < h\nu < 100\,\mathrm{eV}$) or (soft) X-rays ($0.1\,\mathrm{keV} < h\nu < 10\,\mathrm{keV}$). EUV photons can ionize hydrogen atoms in the surface disc layers, creating a nearly isothermal ($\sim 10^4\,\mathrm{K}$) atmosphere which is sharply separated from the neutral gas. The EUV heating rate is rather insensitive to the incident spectrum and thus the integrated mass-loss rate depends mostly on the EUV photon rate, typically resulting in mass-loss

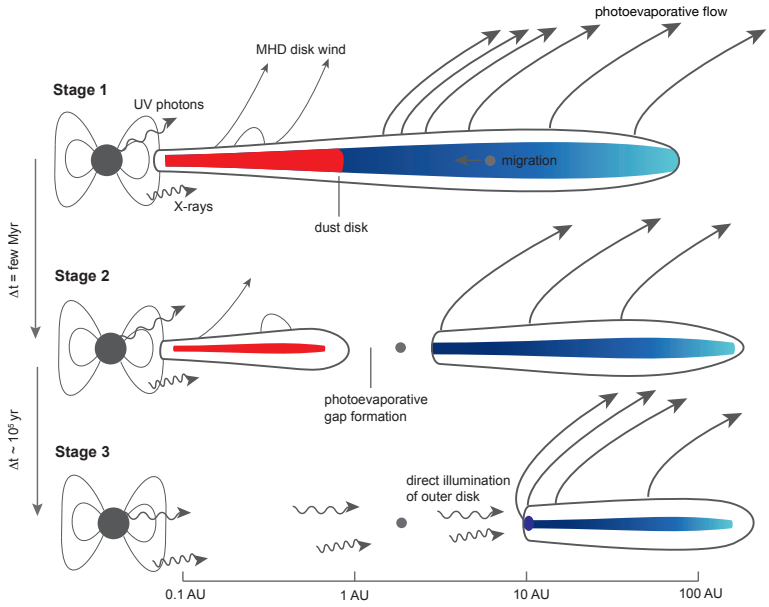

Figure 1.2: Schematic view of the three main stages of disc evolution and dispersal, adapted from Ercolano & Pascucci (2017), which is based on Alexander et al. (2014).

rates of the order of $10^{-10}\,M_\odot\,\mathrm{yr}^{-1}$. EUV photons are fully absorbed within a relatively small neutral hydrogen column $N_\mathrm{H} \approx 10^{20}\,\mathrm{cm}^{-2}$ (Hollenbach & Gorti 2009; Gorti & Hollenbach 2009), making it difficult to constrain the ionizing photon fluxes. Nevertheless, data suggest the rates to be generally low, with the mass loss being concentrated around R_g. EUV photoevaporation is thus ineffective in removing outer disc material and seems to be less important as a driver of disc dispersal until the later stages when the inner disc has already drained. FUV radiation is capable of dissociating H_2 molecules and creates a neutral atomic layer (the energies are too low to ionize the hydrogen atoms). FUV photons show larger penetration depths ($N_\mathrm{H} \approx 10^{21} - 10^{23}\,\mathrm{cm}^{-2}$) than EUV photons, which is however strongly influenced by the abundance of small dust grains and polycyclic aromatic hydrocarbons (PAHs; Alexander et al. 2014; Ercolano & Pascucci 2017). As a consequence, they can drive stronger winds with the mass-loss rates increasing to $10^{-8}\,M_\odot\,\mathrm{yr}^{-1}$ (Gorti & Hollenbach 2009). Also, the mass-loss profile is qualitatively different: While it still peaks around R_g, significant mass loss is also established at large radii beyond 100 au. This opens the possibility for secondary gaps and FUV photoevaporation models sometimes even predict a reversed outside-in clearing (Gorti et al. 2015). Stellar X-rays arise from the magnetically confined hot plasma in the stellar corona and are predominantly absorbed by the K-shells of heavy elements such as oxygen or carbon, releasing photoelectrons that can ionize and heat the gas disc (Alexander et al. 2014). Similar to FUV, X-rays can efficiently deposit energy up to columns of $N_\mathrm{H} \approx 10^{21} - 10^{22}\,\mathrm{cm}^{-2}$. They show a broad wind profile and drive mass-loss rates of the order of $10^{-8}\,M_\odot\,\mathrm{yr}^{-1}$,

depending on the spectral shape and total X-ray luminosity L_X (Owen et al. 2010, 2011, 2012). For young stars, high X-ray luminosities around $10^{30}\,\mathrm{erg\,s^{-1}}$ are typically observed (e.g., Preibisch & Feigelson 2005; Preibisch et al. 2014).

1.2.3 Transition discs

One particularly interesting subgroup of YSOs is represented by the so-called transition discs. They are characterized by inner regions depleted in dust (and possibly gas) and were first identified observationally through a lack of infrared excess in the SED of some YSOs. The launch of the *Spitzer* Space Telescope (*Spitzer*) in 2003 opened up the possibility to observe a large sample of discs with a broad coverage of infrared wavelengths. *Spitzer* studies targeting Class II and Class III objects revealed that a fraction of discs ($\sim 10\,\%$; e.g., Skrutskie et al. 1990) are marked by a lack of near-infrared (NIR) and mid-infrared (MIR) excess while still showing an excess of emission at longer wavelengths, indicating that optically thick emission is coming from an outer disc. Besides these classical transition discs with a hole reaching all the way to the central star, also sources labelled as 'pre-transitional' were detected (Espaillat et al. 2007). The latter are characterized by a NIR excess, but a lack of emission in the MIR. This suggests that an optically thick disc is still present in both the inner and outer disc, which are separated by an annular gap. In Fig. 1.3, examples of the SED of a pre-transitional and transition disc, compared to the median SED (representing a continuous disc) in the Taurus star-forming region, are shown alongside a schematic view of the different groups.

Observations have shown that transition discs appear to be a diverse group of objects, making it difficult to settle on a single definition, and further suggesting different formation routes. Initially classified solely based on their SED, they were thought to be on the verge of dispersal, with their low occurrence pointing towards a short dispersal timescale. Photoevaporation naturally accounts for the formation of transition discs, but models have failed to explain those discs with large holes and simultaneously vigorous accretion (e.g., Owen et al. 2011; Ercolano & Pascucci 2017; Picogna et al. 2019). Detailed observations of transition discs became especially available with the arrival of ALMA and showed that they come with a variety of substructures such as rings, gaps, and spiral or azimuthal asymmetries. While some of the transition discs may represent an intermediate (transitioning) state between an optically thick (full) disc and disc dispersal, dynamical clearing by a massive companion represents an alternative explanation: At least some of the cavities – and in particular the very deep ones – are expected to be the result of such processes rather than representing an evolutionary state. Transition discs, therefore, represent ideal laboratories to probe disc evolution as well as planet-formation models and may enable us to catch planet formation in action.

1.2.4 Planet formation

Planets are built from the dust and gas in protoplanetary discs, starting from the micron-sized grains that are inherited from the interstellar medium (ISM). Thus,

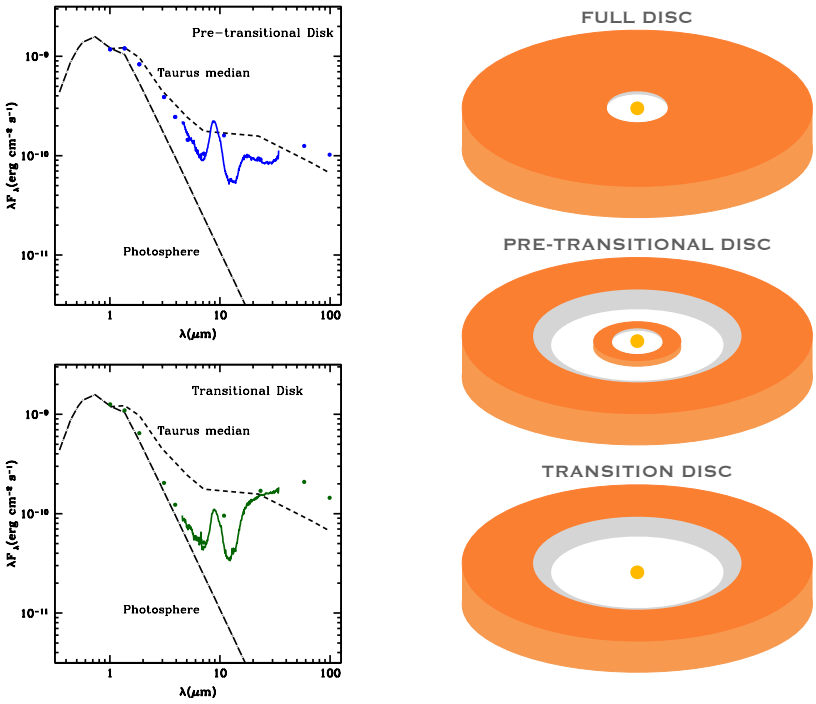

Figure 1.3: Left: SED of a pre-transitional disc (Espaillat et al. 2007) and a transitional disc (Calvet et al. 2005) relative to the Taurus median SED (D'Alessio et al. 1999), as shown in Espaillat et al. (2014). Right: Schematic view of a full, pre-transitional, and transition disc.

planet-formation models must account for the grains to grow by at least 13 orders of magnitude (for recent reviews, see e.g., Johansen & Lambrechts 2017; Izidoro & Raymond 2018; Drazkowska et al. 2022). Both theoretical research (e.g., Wada et al. 2008; Paszun & Dominik 2009; Birnstiel et al. 2010, 2012; Krijt & Kama 2014; Krijt et al. 2015) and laboratory experiments (e.g., Blum & Wurm 2008; Güttler et al. 2010; Kothe et al. 2010; Weidling et al. 2012; Blum et al. 2014) have shown that in the beginning, the dense disc environment allows grains to efficiently stick together in collisions and form millimetre- or even centimetre-sized particles, also called pebbles. This is supported by observations of the different dust size distributions with e.g., ALMA, which further indicate that grain growth already happens on a relatively short timescale of $\sim 10^5$ yr (Harsono et al. 2018).

One limiting factor of grain growth is fragmentation. As the particles grow, the relative velocities at which they impact increase (e.g., Brauer et al. 2008) and at values great than $\sim$1–10 m s^{-1} (e.g., Dominik & Tielens 1997; Blum & Wurm 2008; Wada et al. 2008; Gundlach et al. 2011) the grains tend to fragment or bounce instead of sticking together upon collision. The exact threshold between growth and fragmentation, also called fragmentation velocity, depends on numerous factors, including disc properties such as turbulent mixing or vertical settling, and

grain properties such as grain composition, shape, and surface. For example, the presence of an icy mantel on the grain surface increases the fragmentation velocity and allows for a more efficient grain growth (e.g., Wada et al. 2008; Gundlach et al. 2011).

Another obstacle to the formation of larger bodies beyond the centimetre-sized pebbles is the radial drift barrier. In the beginning, the dust grains are small enough to be well coupled to the gas, which is supported by a pressure gradient and thus rotates at a slightly sub-Keplerian speed. As the grains grow, they decouple from the gas more and more and since they are not supported by pressure they move at Keplerian velocities. Consequently, the particles constantly experience a 'headwind' from the slower-moving gas, which causes them to lose angular momentum and drift inwards. This process can be very fast, causing particles to drift towards the host star within a few 100 years without having the time to grow planets (Whipple 1972; Weidenschilling 1977). The timescale on which the drifting occurs strongly depends on the grain size, mass, and also the density of the surrounding gas and can be quantified with the Stokes number or dimensionless stopping time. The Stokes number is given by the ratio of the stopping and the dynamical timescale. While very small particles, which are dragged with the gas, have Stokes numbers much smaller than one, large metre-sized bodies have Stokes numbers much bigger than one and their transfer of angular momentum to the gas is negligible, thus both of these regimes are not strongly affected by radial drift. The grains with sizes in between (0.1 mm – 1 m) show Stokes numbers around one and experience the strongest gas drag, causing them to quickly spiral towards the star.

A mechanism to overcome the radial drift barrier is the trapping of pebbles in so-called pressure bumps, regions of enhanced density that create a local pressure maximum (Pinilla et al. 2012a,b). Different, not mutually exclusive, mechanisms can account for the presence of such dust traps, including vortices, MRI, spirals in self-gravitating discs, dead zones, and snowlines, but also the outer edge of a gap created by a massive planet. Inside the pressure bumps, particles have the time to grow into metre- or kilometre-sized planetesimals (for a review, see e.g., Pinilla & Youdin 2017). Dust traps are an explanation for the commonly observed ring-like structures in protoplanetary discs, e.g., with ALMA (Andrews 2020).

Following the growth of km-sized planetesimals, gravity starts to dominate the planet-formation process. In this context, planetesimals can either grow through collisions, which can also result in fragmentation (Kokubo & Ida 1996; Tanaka & Ida 1999), or through the accretion of the remaining pebbles (Ormel & Klahr 2010; Lambrechts & Johansen 2012). During a phase of runaway accretion, planetary embryos are formed, with the largest bodies growing the fastest. These planetary embryos later form rocky planets or, if a planetary core has sufficiently grown ($\sim 10\,M_{\mathrm{Earth}}$), accrete the surrounding gas from the disc to form giant planets (e.g., Pollack et al. 1996). Forming such massive cores within the disc's lifetime through planetesimal collisions has been shown to be difficult, especially in the outer disc regions (e.g., Thommes et al. 2003). Pebble accretion on the other hand represents a much faster route to grow these cores once enough planetesimals are formed. Besides the core accretion scenario, an alternative mechanism to form gas

giants is gravitational instability: Similar to the formation of stars, a sufficiently massive and cold disc can become unstable and undergo a gravitational collapse (Boley 2009). This process tends to form very massive planets, or even companion stars rather than planets (e.g., Kratter et al. 2010), at large orbital distances. Through migration processes, these planets can however end up closer to the star.

The onset of planet formation remains an active topic of research, but more and more studies suggest that it starts already in the embedded phase. Evidence of grain growth has been found in protostellar envelopes (Kwon et al. 2009; Miotello et al. 2014; Harsono et al. 2018) and the majority of protoplanetary discs are observed to not have sufficient material to form planetary systems (Ansdell et al. 2016; Manara et al. 2018), even though the disc mass may be underestimated. Young systems on the other hand appear to be massive enough (Tychoniec et al. 2018).

1.3 Disc observations

While evidence for circumstellar material was found already in early times, for example in optical emission spectra (Herbig 1950) or as an excess of emission in the infrared (Ney et al. 1973), it was not until the early 1990s that protoplanetary discs were observed with the *Hubble* Space Telescope (HST) in the Orion Nebula Cluster at optical wavelengths (O'dell & Wen 1994; O'dell & Wong 1996). In the following, discs were also studied in the millimetre-regime with instruments such as the IRAM Plateau de Bure observatory (now NOEMA) or the Submillimeter Array (SMA). Altogether, these observations revealed flat structures around newborn stars, and only with the recent advancement of ALMA and the Spectro-Polarimetric High-contrast Exoplanet REsearch (SPHERE) on ESO's Very Large Telescope(VLT), the door was opened to resolve circumstellar discs at high spatial and spectral resolution. In Fig. 1.4, an HST image of a protoplanetary disc in the Orion Nebula is shown alongside the first ALMA image of the HL Tau disc, highlighting how ALMA has revolutionized the field.

1.3.1 ALMA

The cold ($20 - 50\,\mathrm{K}$) molecular gas of protoplanetary discs emits predominantly at millimetre wavelengths through rotational lines, which can easily be excited at such temperatures, and millimetre-sized grains make up an important contributor in the dust distribution. To study discs in the millimetre-regime, the Atacama Large Millimeter/submillimeter Array (ALMA), an interferometer located in the Atacama desert of the Chilean Andes at a height of about 5000 m, represents the most suited facility. With 66 ($54\times12\,\mathrm{m}$ and $12\times7\,\mathrm{m}$) antennas, operating in 10 Bands that cover wavelengths between 0.3 and 3.6 mm, and possible configurations with baselines ranging from 160 m up to 16 km, ALMA provides both the sensitivity and high resolution to detect faint molecular emission and resolve substructures in the gas as well as the dust, which are further described in the following. Aside from detailed studies of individual sources, ALMA has also allowed for large sur-

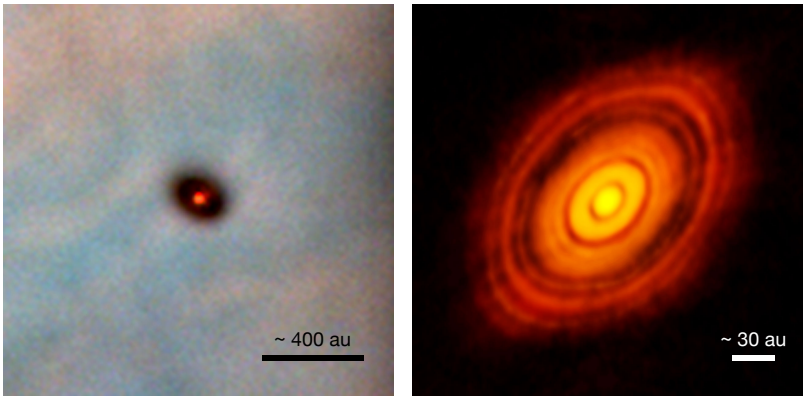

Figure 1.4: Left: Optical HST image of a protoplanetary disc in the Orion Nebula Cluster. Credit: Mark McCaughrean (MPIA), C. Robert O'Dell (Rice University), and NASA/ESA. Right: ALMA image of the HL Tau disc at millimetre wavelengths. Credit: ALMA (ESO/NAOJ/NRAO).

veys, including comprehensive observations of different star-forming regions (e.g., Pascucci et al. 2016; Barenfeld et al. 2016, 2017; Ansdell et al. 2016, 2017; Cox et al. 2017; Long et al. 2017, 2018, 2019; Ward-Duong et al. 2018; Cazzoletti et al. 2019; Cieza et al. 2019; Williams et al. 2019). These population studies have enabled scientists to link important disc properties such as the disc size or mass to the properties of the host star (e.g., Manara et al. 2022; Miotello et al. 2022), which has important implications on the disc evolution and planet-formation processes. They have further shown that the average protoplanetary disc is very different from the largest and brightest discs, which are usually targeted in individual observations.

1.3.2 Dust substructures

Emission from the dust in protoplanetary discs is expected to be brightest at millimetre wavelengths, as millimetre-sized grains dominate the dust population for Class II sources. In this context, the thermal radiation coming from cold dust particles is determined by the particle size, which is comparable to the observed wavelength (Draine 2006). Furthermore, the emission in the millimetre-regime is mostly optically thin and traces dust grains close to the midplane of the disc, where planet formation takes place. Thus, ALMA represents the ideal facility to probe the bulk of the dust content, study dust substructures in the planet-formation region, and search for signposts of planet–disc interactions.

In contrast to the smooth and symmetric structures observed prior to ALMA, high-resolution ALMA observations over the past decade have revealed that a variety of substructures such as gaps or cavities, rings, spiral arms, and azimuthal asymmetries are ubiquitous in the dust component (e.g., van der Marel et al. 2013; Andrews et al. 2018; Cazzoletti et al. 2018; Long et al. 2018; Andrews 2020; Öberg

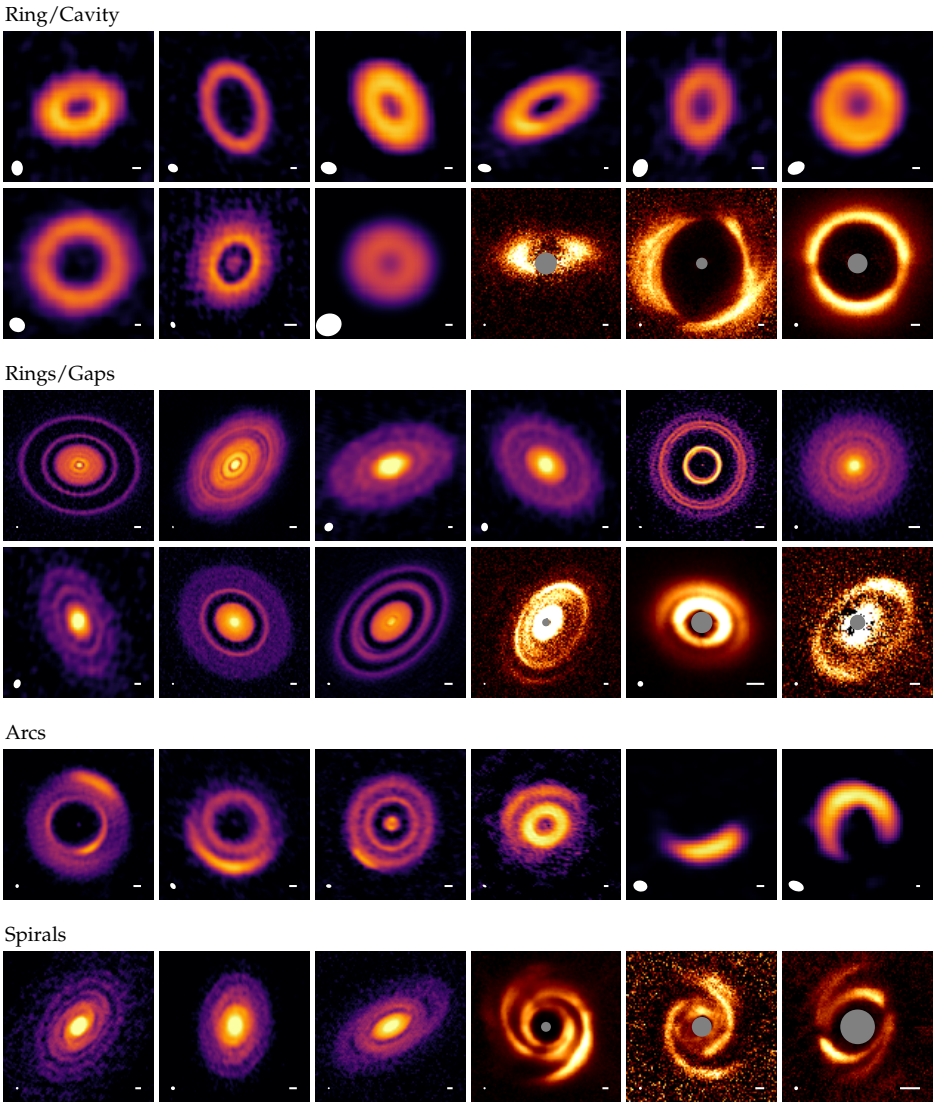

Figure 1.5: Overview of the dust substructures observed at high resolution with ALMA and VLT/SPHERE (indicated by different colormaps), as presented in Andrews (2020).

et al. 2021; Bae et al. 2022; Benisty et al. 2022). Examples of such structures are shown in Fig. 1.5. Also included here are near-infrared scattered light images, which trace the μm-sized grains in the surface disc layers, where spiral structures are particularly well pronounced.

While an interplay of various mechanisms such as photoevaporation (e.g., Owen et al. 2011; Picogna et al. 2019), gravitational instabilities (e.g., Kratter & Lodato 2016), magnetorotational instabilities (e.g., Flock et al. 2015, 2017; Riols & Lesur

2019), zonal flows (e.g., Uribe et al. 2015), or compositional baroclinic instabilities (e.g., Klahr & Bodenheimer 2004) may be responsible for the observed substructures, at least some of them are expected to be the result of dynamical interactions with (massive) planets. Planets are capable of carving gaps in the gas (as the tidal forces will result in a redistribution of angular momentum), producing local pressure maxima which, as previously mentioned, can efficiently trap the dust particles into rings (Lin & Papaloizou 1979). For very massive planetary or binary companions, an entire cavity may be cleared. Planets are further capable of triggering the Rossby-Wave instability (Lovelace et al. 1999; Li et al. 2000, 2001) which creates so-called vortices, i.e., high-pressure dust trapping regions, that can explain the observed azimuthal asymmetries. Theoretical work and simulations have shown that planets can also generate spiral arms (e.g., Ogilvie & Lubow 2002; Rafikov 2002; Dong et al. 2015, 2016; Bae & Zhu 2018a,b).

1.3.3 Gas substructures

In terms of mass, the bulk of the disc material is made up of molecular gas rather than dust, which is not only more difficult to observe due to lower intensities but also not as straightforward to interpret: Molecular emission does not only depend on the gas density but also on its abundance, which is strongly affected by the physical properties of the disc and the chemical reactions taking place therein. Moreover, the most abundant molecule in the gas phase is molecular hydrogen (H_2) which lacks a permanent electric dipole moment, making the detection of H_2 emission extremely challenging. Instead, ALMA observations of the gas content often focus on the second most abundant molecule carbon monoxide (CO), which is marked by a relatively simple and stable chemistry.

Lines from the main isotopologue ^{12}CO are optically thick in most disc regions and thus they trace material emitting from the upper layers of the disc. These are close to the layers probed by the small dust grains in NIR scattered light and are therefore more likely to show spiral substructures. Observations of the latter have for example been observed by Teague et al. (2019b) and are further investigated in Chapters 3, 4, and 5. In the context of planets, spiral features can be explained as follows: The spiral wakes excited by a companion result in an increased surface density and thus higher opacity which moves the $\tau = 1$ layer to a higher altitude where the temperature is generally higher (Phuong et al. 2020a,b). To trace disc layers which are closer to the midplane, less abundant isotopologues such as ^{13}CO, C^{18}O, or also C^{17}O, ^{13}C^{17}O (Booth et al. 2019), and ^{13}C^{18}O are needed. While these molecules are even more difficult to observe with sufficient sensitivity, they are more likely to provide information about annular substructures such as gaps or cavities. The latter have indeed been confirmed by several observations (e.g., Perez et al. 2015a; van der Marel et al. 2016; Dong et al. 2017; Ubeira Gabellini et al. 2019).

Besides CO, which is marked by a relatively easy and well-understood chemistry, also other molecules, such as CN, CS, C_2H, HCO^+, DCO^+, N_2H^+ just to name a few, are interesting to study both through modelling and observations, as each molecule provides unique information about the physical properties of the

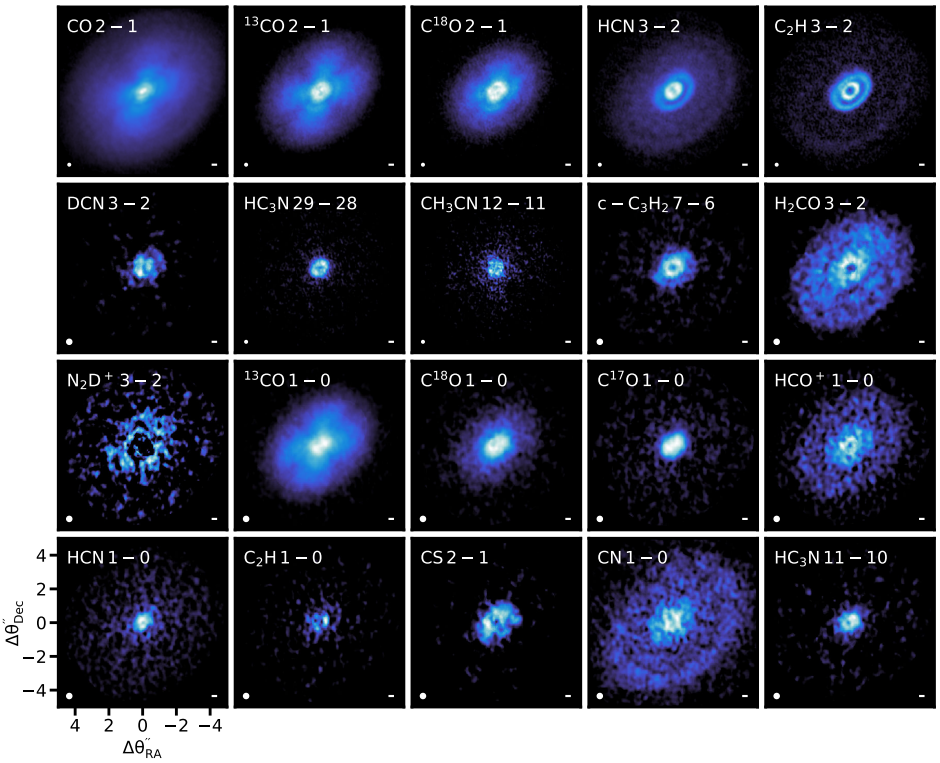

Figure 1.6: Gallery of the MAPS observations of the HD 163296 disc. Shown are the Moment 0 maps of 20 lines targeted with ALMA. Adapted from Öberg et al. (2021).

disc and the underlying chemistry. A comprehensive ALMA study of the chemical inventory of protoplanetary discs was recently performed within the MAPS program (Molecules with ALMA at Planet-forming Scales; Öberg et al. 2021), showing an impressive diversity in the abundances, distributions, and substructures of the molecules. A gallery of the MAPS observations is shown in Fig. 1.6 for the HD 163296 disc.

In contrast to the dust, gas emission includes information on the dynamics – or kinematics – in protoplanetary discs, as the lines emitted by rotating gas are red- and blueshifted depending on whether the material is moving towards or away from the observer. This opens up a unique new window to study the mechanisms being at play in discs. Disc kinematics represent a key topic of this thesis and are therefore described in more detail in the following section.

1.4 Kinematics

Ultimately, only a direct detection of a young planet can confirm the link between the observed gas and dust substructures and planet formation. However, the

dense and opaque environment surrounding young planets makes such a task very challenging and feasible only for the most massive and bright planets that are less affected by dust extinction (Sanchis et al. 2020). To date, the only robust detection of embedded (several $M_{\rm J}$-sized) planets and their circumplanetary discs are those of the PDS 70 system (Keppler et al. 2018; Haffert et al. 2019; Benisty et al. 2021). This has triggered the development of other more indirect detection techniques.

Among these methods, a particularly promising one is to study the velocity field of the rotating gas, observed through molecular line emission. Deviations from purely Keplerian rotation (as expected of unperturbed gas) yield information about the processes shaping the disc (see Pinte et al. 2022 for a review). For detailed studies of kinematical substructures, a high spectral resolution is essential ($\sim 50\,\mathrm{m\,s^{-1}}$), and a relatively high spatial resolution is preferred ($< 0\farcs1$). While such observations are accessible with ALMA they come at high observational costs, thus this field remains in its infancy and the number of sources for which the kinematics have been thoroughly observed and analysed is limited.

Under the assumption that the disc is in both radial and vertical hydrostatic equilibrium and that the gravity is dominated by the central star, the rotation velocity can be written as

$$\frac{v_\phi^2(r,z)}{r} = \frac{GM_* r}{(r^2+z^2)^{3/2}} + \frac{1}{\rho_{\rm gas}}\frac{\partial P_{\rm gas}}{\partial r}, \tag{1.3}$$

where $\partial P_{\rm gas}/\partial r$ is the radial pressure gradient (Rosenfeld et al. 2013). Self-gravity is neglected in Eq. 1.3. Quantifying deviations from the rotation velocity can thus be used to trace perturbations in the pressure gradient, for example induced by a planet, which causes a negative gradient inside and a positive one outside of its orbit (Kanagawa et al. 2015; Teague et al. 2018a).

For a given frequency, line emission is concentrated in a region of constant projected velocity, also called isovelocity curve. Due to the Keplerian rotation of the disc, these channels follow a 'butterfly' pattern (Horne & Marsh 1986; Beckwith & Sargent 1993). The nature of the velocity field was shown through earlier observations (e.g., Dutrey et al. 2014b), however, ALMA's high spatial resolution opened the possibility to resolve and separate emission from both the upper (above the midplane) and the lower (below the midplane) disc surfaces. Channel maps, which are relatively noisy, can be collapsed into a map displaying the full rotation field. In this context, different methods have been used such as the integration over the spectral axis to obtain the intensity weighted average velocity or Moment 1 map, fitting of a Gaussian profile (Casassus & Pérez 2019) or double Gaussian profile (Casassus et al. 2021; Izquierdo et al. 2022), or the quadratic method introduced by Teague & Foreman-Mackey (2018). While collapsing a cube into a rotation map brings the advantage of an increased signal-to-noise ratio (SNR), it washes out the distinction between the upper and lower disc surfaces.

Both the velocity channels and rotation maps directly reflect the underlying gas velocity and for a non-perturbed Keplerian disc they are expected to be smooth. Perturbations to the velocity on the other hand result in visible features that can be analysed by modelling the rotation velocity. Two methods are used in this

thesis to study disc kinematics, one modelling the rotation map (Chapters 3 and 4) and the other modelling the channel maps (Chapter 5). The former approach is relatively straightforward: The projected line-of-sight velocity is given by

$$v_{\phi,\mathrm{proj}}(r,\phi) = v_\phi(r)\cos\phi\sin i, \tag{1.4}$$

where ϕ is the polar angle and i the inclination of the disc. To deproject the sky-plane coordinates (x, y) into the disk-frame coordinates (r, ϕ), information of the disc geometry, namely the source centre, inclination, position angle, and height $z(r)$ of the emission surface, can be used based on the assumption of axisymmetry (Rosenfeld et al. 2013). These parameters can then be left free to find the best-fitting parameters for a given model of v_ϕ (e.g., as in Eq. 1.4). To fit the rotation map, this thesis uses the EDDY package, presented in Teague (2019). In the second approach, the channel maps are fitted individually. This method was recently introduced by Izquierdo et al. (2021) as the DISCMINER tool. In the DISCMINER, parametric prescriptions are adopted to reproduce the line profiles in each channel, with the intensity being described by a generalized bell kernel. This approach has the advantage that the upper and lower emission surfaces can be modelled simultaneously. It further retrieves information on the line width, which is not accessible through the first method. With the DISCMINER, localized velocity perturbations can be identified both in radius and azimuth.

While the different mechanisms taking place in the disc will all leave their individual fingerprints in the kinematics, with their exact contribution and morphology yet to be disentangled, kinematical features of planet–disc interactions are particularly exciting and outlined in the following.

1.4.1 Kinematical signatures of planets

Planets have been found to excite spiral density waves at Lindblad resonances just outside their orbit (Goldreich & Tremaine 1979, 1980; Papaloizou & Lin 1984), which can manifest in a one-armed spiral structure, called the planet wake (Ogilvie & Lubow 2002). This disturbs the density structure of the disc but also the velocity field and can result in significant azimuthal deviations from Keplerian rotation (up to a few 10 %) and radial motions (e.g., Bollati et al. 2021), with the azimuthal deviations being largest near the planet location and the radial motions dominating at large distances from the wake (Rafikov 2002). The planetary wake also triggers vertical motions in the form of meridional eddies (Fung & Chiang 2016). The exact amplitude of the perturbation strongly depends on the planetary mass, but also the disc structure. In addition to the Lindblad spirals, planets can launch buoyancy spirals under certain thermal conditions (e.g., Zhu et al. 2012, 2015; Lubow & Zhu 2014; McNally et al. 2020). These spirals appear to be much more tightly wound, especially close to the location of the planet, and predominantly trigger vertical motions, thus both types of spirals produce distinctive kinematical features. Non-Keplerian spirals have been observed in the gas disc of several sources: TW Hya (Teague et al. 2019b), HD 100453 (Rosotti et al. 2020a), HD 135344B (Casassus et al. 2021), HD 163296 and MWC 480 (Teague et al. 2021), HD 142527 (Garg et al. 2021), and J 1604 (Stadler et al. 2023) are all marked by spiral substructures.

Chapters 3, 4, and 5 further explore the kinematical spirals in a number of sources. Another signature of a spiral wake, the so-called Doppler-flip, a sign reversal in the non-Keplerian velocity component, has been reported in the HD 100546 disc by Casassus & Pérez (2019); Casassus et al. (2022), with its planetary origin, however being debated (Norfolk et al. 2022). A detailed kinematical analysis of the protoplanetary disc around HD 100546 is conducted in Chapter 5.

As previously mentioned, planets are capable of carving an annular gap in the disc, resulting in steep pressure gradients at the edges and a sub-Keplerian flow at the inner and super-Keplerian flow at the outer edge. It is however important to note that, depending on the planetary mass, a gap may be visible in the dust while the gas profile is only slightly affected (Dipierro et al. 2016) and deviations from Keplerian rotation may not be observed around a dust gap. Furthermore, a gas density gradient may be hidden in deep cavities, where the opacity is reduced and consequently the temperature gradient becomes the dominating factor (Rab et al. 2020). Deviations in the rotation profile, likely tracing pressure gradients in gas gaps, have been measured by Teague et al. (2018a) in HD 163296. From the edges of a gas gap, material (viscously) moves towards the gap centre and the midplane, creating significant motions also known as meridional flows (Kley et al. 2001; Tanigawa et al. 2012; Szulágyi et al. 2014; Morbidelli et al. 2014), which have been observed in the kinematics (Teague et al. 2019a; Yu et al. 2021). These ordered flows are not exclusive to planet-induced gaps and studying their azimuthal variations provides insights into the underlying mechanisms that formed the gap. In addition, planets can trigger turbulent motions, which result in a local enhancement of line width (Dong et al. 2019). These motions, even though hard to detect, can further help to distinguish between a planet and other gap-opening processes.

An embedded planet perturbs the gas flow in such a way that an additional Doppler shift is induced in the molecular emission, which manifests in the channel maps as a distortion of the iso-velocity curve, also referred to as 'kinks' or 'wiggles'. Kink-features that are in agreement with planets of several $M_{\rm J}$ have been observed in HD 163296 and HD 97048 (Pinte et al. 2018b, 2019), tentative detections were identified by Pinte et al. (2020) in eight of the DSHARP sources (Andrews et al. 2018), as well as in CI Tau (Rosotti et al. 2021). Modelling of the channel maps of HD 163296 with the DISCMINER yielded strong indications for two embedded planets (Izquierdo et al. 2022). A localized kinematic structure was detected in atomic carbon of the same disc (Alarcón et al. 2022). On top of that, the presence of a circumplanetary disc (CPD) – an accretion disc which channels material onto a sufficiently massive planet – can cause a spot in the channels which is detached from the iso-velocity curve of the parent disc: The gas flow onto the planet adds a significant velocity distortion and under certain conditions (e.g., certain respective disc orientations), the CPD emission can decouple from the emission of the background disc (e.g., Perez et al. 2015b). A summary of the expected kinematic signatures in a planet-forming disc is presented in Fig. 1.7.

Altogether, kinematical observations open the opportunity to find embedded planets which escape the classical detection techniques and yield important implications on the planet-formation processes. Knowledge of the planetary location

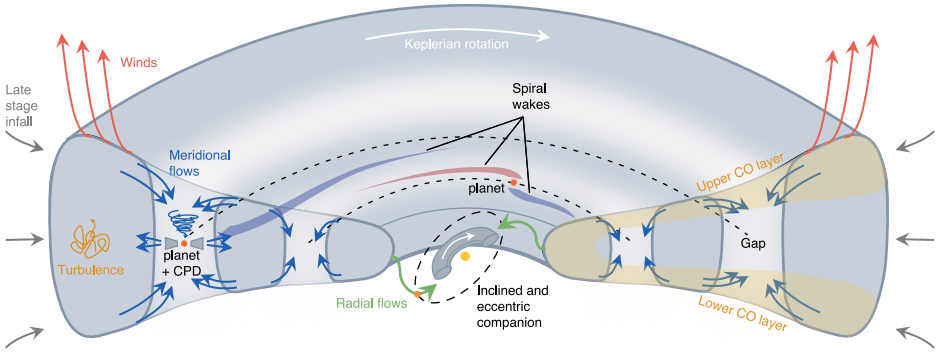

Figure 1.7: Schematic view of the possible kinematic signatures, exhibited by a planet-forming disc. Adapted from Pinte et al. (2022)

and mass is crucial to put constraints on the current planet-formation models (such as gravitational instability or pebble accretion). Linking kinematical signatures with the location of dust gaps provides information about the onset of planet formation, as planet-carved gaps indicate that the planet formation has already reached an advanced stage. This suggests that the timescales in which planets are formed are even shorter than previously thought or that some migration processes have already taken place. By increasing the database of detected young planets, kinematical studies bring the potential of population studies to understand possible patterns and link them to the properties of mature exoplanet populations.

1.5 This thesis

In the last decade, ground-breaking facilities such as ALMA and SPHERE have revolutionized the field of planet formation: With high angular resolution observations of the circumstellar material, it is now possible to uncover numerous and diverse substructures that are exhibited by discs. The interpretation of these substructures is however not straightforward, as different mechanisms, often being at play simultaneously, are shaping the disc. Three key questions have been triggered:

1. Are these substructures the result of planet–disc interactions or other mechanisms?

2. If planets are the cause, what can we learn about these planets, for example in terms of location or mass, and if not planet-driven, what can we learn about the disc?

3. What modulates angular momentum transport in the disc as well as disc dispersal, influencing the disc lifetime and thus the time to build planets?

This dissertation focuses on interpreting disc substructures in the context of disc winds as well as planet–disc interactions by using different modelling and obser-

vational techniques. It contributes to the understanding of how common they are, if they follow certain patterns and if differences or similarities can be identified for different disc populations. A special focus is set on transition discs, which represent ideal laboratories to observe planet formation in action and test disc evolution models. The individual chapters and their conclusions are summarized as follows:

Chapter II: Photoevaporative disc winds in carbon-depleted discs

One mechanism able to explain the formation of gaps and cavities in discs is photoevaporation, however, it can not account for the observed diversity of transition discs and especially fails at explaining discs with large cavities and simultaneous strong gas accretion. This chapter investigates photoevaporative winds acting in discs in which, as commonly observed, volatile carbon is depleted, and how they affect the formation of cavities. For this purpose, radiative transfer and hydrodynamical models are combined. The results show that (X-ray) photoevaporative winds are, with respect to solar metallicity discs, stronger in such carbon-depleted discs, resulting in enhanced mass-loss rates and mass-loss profiles extending to larger radii. These results may explain a larger number of the observed transition discs. Additionally, very high carbon depletion may represent a mechanism of very fast disc dispersal towards the end of the disc's lifetime.

Chapter III: Spiral structures in the gas disc of CQ Tau

In the last decade, high-angular-resolution observations have shown that circumstellar discs are marked by a variety of substructures, triggering the question of whether they are caused by planet–disc interactions. In this chapter, both the kinematics and brightness temperatures of the disc around CQ Tau are analysed using high-resolution CO observations taken with ALMA. To search for deviations from Keplerian rotation and variations in the temperature structure, a Keplerian disc model is fitted to the velocity field. The results yield significant spiral features in both the gas velocity and brightness temperature residuals, which together with spirals observed in the near-infrared and a detected deep gas and dust cavity point towards ongoing giant planet formation in the disc.

Chapter IV: A survey of the kinematics and brightness temperatures of transition discs

To interpret the origin of the various substructures exhibited by protoplanetary discs, it is crucial to understand how common they are and if they follow certain patterns. In this chapter, the analysis conducted in Chapter III is expanded to a sample of 36 large cavity transition discs, pushing the available ALMA observations to their limits. For the analysis, archival CO data are used, taken in Band 6 and Band 7. For the first time, the substructures found in the kinematics and brightness temperature are compared to other indicators for the presence of planets for a large sample of sources. The results yield strong features such as arcs or spirals, possibly associated with the presence of planets or companions, in about 20 % of discs, while the

majority of the sources do not present as clear signatures. Almost all discs that exhibit spirals in near-infrared scattered light show at least tentative features in the CO data.

Chapter V: Spirals and meridional flows in the planet-forming disc around HD 100546

The disc surrounding the Herbig star HD 100546 represents a particularly interesting target to search for planet–disc interactions, as numerous direct and indirect evidence for ongoing planet formation has been observed in both the dust and gas emission. In this chapter, a multi-line analysis of the gas kinematics is conducted, using several CO lines observed in Band 6, 7, and 10 with ALMA. To model the line emission for each intensity cube, the DISCMINER package is used. The analysis reveals extended spiral structures in the kinematics of all lines, whose overall morphology is well reproduced by linear and logarithmic functions. They are consistent with spirals driven by an embedded companion – either planetary or binary – inside of 50 au. The pitch angles of the spirals decrease towards the midplane, which is in agreement with theoretical predictions for a dynamical interaction scenario. Indications of a second companion located further out between 90-150 au are seen in the form of meridional flows towards the midplane and pressure minima, as well as a tentative gap in the more optically thin tracers. An asymmetry in the emission heights of the blue- and redshifted sides may indicate infalling material on the redshifted side of the disc or an inner warped disc, casting a shadow over the outer disc.

1.5.1 Future outlook

ALMA has transformed our view of planet-forming discs and this thesis provides some first steps in the direction of interpreting their substructures. It further helps to understand which of the sources are the most promising to target with other instruments, dedicated at the search and direct imaging of exoplanets. At the same time, it stresses the importance of even better observations, both in terms of resolution and sensitivity, to really disentangle the different mechanisms being at play in discs and the origin of the substructures remains a burning open question. We have now reached a time where new and exciting opportunities are opening up both with ALMA (e.g., exoALMA large program; PI: R.Teague) and the James Webb Space Telescope (JWST).

While ALMA observations of molecular line emission may not reach the same spatial resolution as achieved for the continuum, they can be used to analyse the gas flow throughout the disc, opening a unique new window to detect embedded planets and probe physical processes in the disc. The field of disc kinematics has just started to emerge and very deep line observations taken at high spectral and spatial resolutions are essential and will allow us to also detect smaller mass planets at shorter periods. Furthermore, a systematic and comprehensive survey of a large number of planet-forming discs, covering a wide range of disc-star system morphologies, will be needed to link the properties of discs and their young planets to the mature exoplanet populations that are observed with an enormous variety.

In this context, it is important to also analyse the smaller discs, generally thought to be less structured, in addition to the massive and bright discs that are typically studied in detail. This is an essential step to understand if there are systematic differences between these groups and if in particular Herbig Ae/Be or T Tauri discs follow different patterns.

So far, mostly the brighter CO lines have been used to map out the disc kinematics. However, to really understand the mechanisms behind the observed substructures it is crucial to trace them throughout the full radial and vertical extent of the disc. This requires deep high-resolution observations of a range of molecular tracers aside from CO, which further brings the opportunity to understand the chemical signatures of planets. To interpret the observations, fundamental work is also required on the theoretical side. Dedicated modelling of both planet–disc interactions and other disc-shaping mechanisms such as disc winds or gravitation instabilities and their imprints on the kinematics and temperature structure is crucial to understand the role that individual processes play in the planet-formation puzzle. Exciting opportunities will also open up with JWST and the Extremely Large Telescope (ELT) to directly image young (proto-)planets, that are responsible for the deviations in the velocity field. In combination with ALMA, these facilities will pave the way for a comprehensive characterization of the youngest exoplanets. Coupling ALMA observations of the overall disc structure with JWST spectroscopy projects, tackling the inner disc structure, will further enable us to access the connection of inner and outer disc structures, which is so far not fully understood.